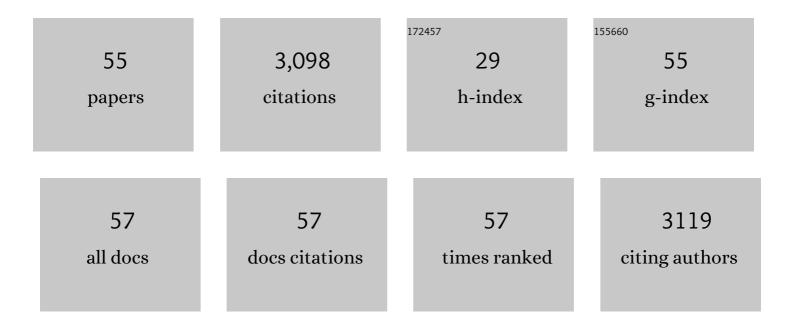
## Stephan M Kraemer

List of Publications by Year in descending order

Source: https://exaly.com/author-pdf/11122069/publications.pdf Version: 2024-02-01



STEDHAN M KDAEMED

#	Article	IF	CITATIONS
1	Iron oxide dissolution and solubility in the presence of siderophores. Aquatic Sciences, 2004, 66, 3-18.	1.5	522
2	lron Isotope Fractionation during Proton-Promoted, Ligand-Controlled, and Reductive Dissolution of Goethite. Environmental Science & Technology, 2006, 40, 3787-3793.	10.0	235
3	Steady-state dissolution kinetics of goethite in the presence of desferrioxamine B and oxalate ligands: implications for the microbial acquisition of iron. Chemical Geology, 2003, 198, 63-75.	3.3	190
4	Effect of siderophores on the light-induced dissolution of colloidal iron(III) (hydr)oxides. Marine Chemistry, 2005, 93, 179-193.	2.3	133
5	Effect of hydroxamate siderophores on Fe release and Pb(II) adsorption by goethite. Geochimica Et Cosmochimica Acta, 1999, 63, 3003-3008.	3.9	128
6	Root exudation of phytosiderophores from soilâ€grown wheat. New Phytologist, 2014, 203, 1161-1174.	7.3	124
7	Iron isotope fractionation in oxic soils by mineral weathering and podzolization. Geochimica Et Cosmochimica Acta, 2007, 71, 5821-5833.	3.9	118
8	Iron isotope fractionation during proton- and ligand-promoted dissolution of primary phyllosilicates. Geochimica Et Cosmochimica Acta, 2010, 74, 3112-3128.	3.9	90
9	Temperature dependence of goethite dissolution promoted by trihydroxamate siderophores. Geochimica Et Cosmochimica Acta, 2002, 66, 431-438.	3.9	86
10	Iron Isotope Fractionation during Pedogenesis in Redoximorphic Soils. Soil Science Society of America Journal, 2007, 71, 1840-1850.	2.2	79
11	Adsorption of Pb(II) and Eu(III) by Oxide Minerals in the Presence of Natural and Synthetic Hydroxamate Siderophores. Environmental Science & Technology, 2002, 36, 1287-1291.	10.0	77
12	Photoreductive Dissolution of Iron(III) (Hydr)oxides in the Absence and Presence of Organic Ligands: Experimental Studies and Kinetic Modeling. Environmental Science & Technology, 2009, 43, 1864-1870.	10.0	76
13	Metallophores and Trace Metal Biogeochemistry. Aquatic Geochemistry, 2015, 21, 159-195.	1.3	76
14	Iron Isotope Fractionation during Fe Uptake and Translocation in Alpine Plants. Environmental Science & Technology, 2010, 44, 6144-6150.	10.0	72
15	Synergistic Effect of Reductive and Ligand-Promoted Dissolution of Goethite. Environmental Science & Technology, 2015, 49, 7236-7244.	10.0	69
16	Bacterial Siderophores Promote Dissolution of UO2under Reducing Conditions. Environmental Science & Technology, 2005, 39, 5709-5715.	10.0	65
17	Iron speciation and isotope fractionation during silicate weathering and soil formation in an alpine glacier forefield chronosequence. Geochimica Et Cosmochimica Acta, 2011, 75, 5559-5573.	3.9	62
18	Influence of pH and Competitive Adsorption on the Kinetics of Ligand-Promoted Dissolution of Aluminum Oxide. Environmental Science & Technology, 1998, 32, 2876-2882.	10.0	59

#	Article	IF	CITATIONS
19	The influence of pH on iron speciation in podzol extracts: Iron complexes with natural organic matter, and iron mineral nanoparticles. Science of the Total Environment, 2013, 461-462, 108-116.	8.0	55
20	Influence of solution saturation state on the kinetics of ligand-controlled dissolution of oxide phases. Geochimica Et Cosmochimica Acta, 1997, 61, 2855-2866.	3.9	54
21	Photolysis of Citrate on the Surface of Lepidocrocite:  An in situ Attenuated Total Reflection Infrared Spectroscopy Study. Journal of Physical Chemistry C, 2007, 111, 10560-10569.	3.1	48
22	ATR-FTIR spectroscopic study of the adsorption of desferrioxamine B and aerobactin to the surface of lepidocrocite (γ-FeOOH). Geochimica Et Cosmochimica Acta, 2009, 73, 4661-4672.	3.9	44
23	An assay for screening microbial cultures for chalkophore production. Environmental Microbiology Reports, 2010, 2, 295-303.	2.4	43
24	Phytosiderophore-induced mobilization and uptake of Cd, Cu, Fe, Ni, Pb and Zn by wheat plants grown on metal-enriched soils. Environmental and Experimental Botany, 2017, 138, 67-76.	4.2	37
25	Structure and reactivity of oxalate surface complexes on lepidocrocite derived from infrared spectroscopy, DFT-calculations, adsorption, dissolution and photochemical experiments. Geochimica Et Cosmochimica Acta, 2018, 226, 244-262.	3.9	37
26	Biogeochemical controls on the mobility and bioavailability of metals in soils and groundwater. Aquatic Sciences, 2004, 66, 1-2.	1.5	34
27	Low Fe(II) Concentrations Catalyze the Dissolution of Various Fe(III) (hydr)oxide Minerals in the Presence of Diverse Ligands and over a Broad pH Range. Environmental Science & Technology, 2019, 53, 98-107.	10.0	34
28	Genome wide transcriptomic analysis of the soil ammonia oxidizing archaeon <i>Nitrososphaera viennensis</i> upon exposure to copper limitation. ISME Journal, 2020, 14, 2659-2674.	9.8	33
29	Magnitude and Mechanism of Siderophore-Mediated Competition at Low Iron Solubility in the Pseudomonas aeruginosa Pyochelin System. Frontiers in Microbiology, 2017, 8, 1964.	3.5	32
30	Low Concentrations of Surfactants Enhance Siderophore-Promoted Dissolution of Goethite. Environmental Science & Technology, 2007, 41, 3633-3638.	10.0	31
31	Photodissolution of lepidocrocite (γ-FeOOH) in the presence of desferrioxamine B and aerobactin. Geochimica Et Cosmochimica Acta, 2009, 73, 4673-4687.	3.9	31
32	Mercury Isotope Fractionation in the Subsurface of a Hg(II) Chloride-Contaminated Industrial Legacy Site. Environmental Science & Technology, 2019, 53, 7296-7305.	10.0	29
33	Synergistic Effects between Biogenic Ligands and a Reductant in Fe Acquisition from Calcareous Soil. Environmental Science & Technology, 2016, 50, 6381-6388.	10.0	27
34	Fe(II)-Catalyzed Ligand-Controlled Dissolution of Iron(hydr)oxides. Environmental Science & Technology, 2019, 53, 88-97.	10.0	26
35	Rate laws of steady-state and non-steady-state ligand-controlled dissolution of goethite. Colloids and Surfaces A: Physicochemical and Engineering Aspects, 2007, 306, 22-28.	4.7	20
36	Wavelength-Dependence of Photoreductive Dissolution of Lepidocrocite (γ-FeOOH) in the Absence and Presence of the Siderophore DFOB. Environmental Science & Technology, 2009, 43, 1871-1876.	10.0	20

#	Article	IF	CITATIONS
37	Microbial decomposition of 13C- labeled phytosiderophores in the rhizosphere of wheat: Mineralization dynamics and key microbial groups involved. Soil Biology and Biochemistry, 2016, 98, 196-207.	8.8	20
38	Copper complexation of methanobactin isolated from Methylosinus trichosporium OB3b: pH-dependent speciation and modeling. Journal of Inorganic Biochemistry, 2012, 116, 55-62.	3.5	19
39	4. Siderophores and the Dissolution of Iron-Bearing Minerals in Marine Systems. , 2005, , 53-84.		17
40	Accurate LCâ€ESIâ€MS/MS quantification of 2′â€deoxymugineic acid in soil and root related samples employing porous graphitic carbon as stationary phase and a <sup>13</sup> C <sub>4</sub> â€labeled internal standard. Electrophoresis, 2014, 35, 1375-1385.	2.4	16
41	Effects of anionic surfactants on ligand-promoted dissolution of iron and aluminum hydroxides. Journal of Colloid and Interface Science, 2008, 321, 279-287.	9.4	14
42	A Simple Assay for Screening Microorganisms for Chalkophore Production. Methods in Enzymology, 2011, 495, 247-258.	1.0	14
43	Isolation and purification of Cu-free methanobactin from Methylosinus trichosporiumOB3b. Geochemical Transactions, 2011, 12, 2.	0.7	13
44	Importance of oxidation products in coumarin-mediated Fe(hydr)oxide mineral dissolution. BioMetals, 2020, 33, 305-321.	4.1	12
45	Copper limiting threshold in the terrestrial ammonia oxidizing archaeon Nitrososphaera viennensis. Research in Microbiology, 2020, 171, 134-142.	2.1	12
46	The Effect of pH and Biogenic Ligands on the Weathering of Chrysotile Asbestos: The Pivotal Role of Tetrahedral Fe in Dissolution Kinetics and Radical Formation. Chemistry - A European Journal, 2019, 25, 3286-3300.	3.3	9
47	Investigation of Siderophore-Promoted and Reductive Dissolution of Dust in Marine Microenvironments Such as Trichodesmium Colonies. Frontiers in Marine Science, 2020, 7, .	2.5	9
48	Ligand-Induced U Mobilization from Chemogenic Uraninite and Biogenic Noncrystalline U(IV) under Anoxic Conditions. Environmental Science & Technology, 2022, 56, 6369-6379.	10.0	8
49	Adsorption of hydroxamate siderophores and EDTA on goethite in the presence of the surfactant sodium dodecyl sulfate. Geochemical Transactions, 2009, 10, 5.	0.7	6
50	Identifying the reactive sites of hydrogen peroxide decomposition and hydroxyl radical formation on chrysotile asbestos surfaces. Particle and Fibre Toxicology, 2020, 17, 3.	6.2	6
51	Linking Isotope Exchange with Fe(II)-Catalyzed Dissolution of Iron(hydr)oxides in the Presence of the Bacterial Siderophore Desferrioxamine-B. Environmental Science & Technology, 2020, 54, 768-777.	10.0	5
52	Soil-pH and cement influence the weathering kinetics of chrysotile asbestos in soils and its hydroxyl radical yield. Journal of Hazardous Materials, 2022, 431, 128068.	12.4	5
53	Copper mobilisation from Cu sulphide minerals by methanobactin: Effect of <scp>pH</scp> , oxygen and natural organic matter. Geobiology, 2022, 20, 690-706.	2.4	5
54	Catalytic effects of photogenerated Fe(II) on the ligand-controlled dissolution of Iron(hydr)oxides by EDTA and DFOB. Chemosphere, 2021, 263, 128188.	8.2	3

#	Article	IF	CITATIONS
55	Siderophores. Encyclopedia of Earth Sciences Series, 2011, , 793-796.	0.1	3